Robotics and Autonomous Systems 57 (2009) 796–807

Contents lists available at ScienceDirect

Robotics and Autonomous Systems

journal homepage: www.elsevier.com/locate/robot

Learning to fall: Designing low damage fall sequences for humanoid soccer robots

J. Ruiz-del-Solar [a,*], R. Palma-Amestoy [a,1], R. Marchant [a,1], I. Parra-Tsunekawa [a,1], P. Zegers [b,1]

[a] Department of Electrical Engineering, Universidad de Chile, Avenida Tupper 2007, Casilla 412-3, Santiago, Chile
[b] College of Engineering, Universidad de Los Andes, Chile

ARTICLE INFO

Article history:
Available online 8 April 2009

Keywords:
Humanoid soccer robots
Full-body motion control
Fall management
Complex humanoid robots simulation
Nao humanoid robots

ABSTRACT

A methodology for the analysis and design of fall sequences of robots that minimize joint/articulation injuries, and the damage of valuable body parts is proposed. These fall sequences can be activated/triggered by the robot in case of a detected unintentional fall or an intentional fall, which are common events in humanoid soccer environments. The methodology is human-based and requires the use of a realistic simulator as development tool. The obtained results show that fall sequences designed using the proposed method produce less damage than standard, uncontrolled falls.

1. Introduction

In soccer, as in many other sports that allow contact among players, it is usual that players fall down, as consequence of fouls, collisions with other players or objects, or extreme body actions, such as fast movements or ball kicks from unstable body positions. In addition, soccer players can intentionally fall down to block the ball trajectory (defense player) or to gain control of the ball (goalkeeper). Therefore, we can affirm that the management of falls—i.e. how to avoid an unintentional fall, how to fall without damaging the body, how to achieve fast recovering of the standing position after a fall—is an essential ability of good soccer players. In general terms, the adequate management of falls is important for any physical human activity.

Given that one of the main goals of robot soccer competitions (RoboCup and FIRA contests) is to allow robots to play soccer as humans do, the correct management of falls in legged robots, especially in highly unstable systems such as biped humanoid robots, is a very relevant matter. However, to the best of our knowledge this issue has almost not been addressed in the robot soccer and other mobile robotics communities. The current situation in robot soccer is that:

(i) In case of an unintentional fall, the standard situation is that robots do not realize they are falling down. Therefore, they do not perform any action for diminishing the fall damage. After the fall, they recognize they are on the ground using their internal sensors, and they start a standing up sequence of movements. There are some few examples of systems that detect unstable situations and avoid the fall [1–4].

(ii) In most cases, unintentional or intentional falls, robots fall as deadweight, without using a fall sequence that allows them to dissipate some of the kinetic energy of the fall or to protect some valuable body parts, as humans do. Two of the few works that address this issue are [5,6], although none of them was developed in the context of robot soccer. In some other works this issue is partially addressed by switching off the robot's motors, once the fall is detected. The idea behind this action is to lower the motor's damage.

(iii) The damage of robot components or parts of the surrounding environment after a fall is a real problem. This is one of the reasons for limiting the size of robots in some robot soccer leagues (e.g. RoboCup TeenSize league).

In this context, the aim of this paper is to address the management of falls in robot soccer. In concrete, we propose a methodology to design fall sequences that minimize joint/articulation injuries, as well as the damage of valuable body parts (cameras and processing units). These fall sequences can be activated/triggered by the robot in case of a detected unintentional fall or in case of an intentional fall. The idea is to take control of the fall, as soon as the robot detects it. The proposed design methodology is iterative, it consists on the application of consecutive synthesis and analysis steps by a human designer, and it makes use of a realistic robot simulator, as a development and evaluation tool.

It is not our intention to cover exhaustively the management of falls in this article, but to propose a methodology for the design of fall sequences and to focus the attention of the community on this important problem.

---

[*] Corresponding author. Tel.: +56 2 978 4207; fax: +56 2 695 3881.
E-mail addresses: jruizd@ing.uchile.cl (J. Ruiz-del-Solar), ropalma@ing.uchile.cl (R. Palma-Amestoy), romarcha@ing.uchile.cl (R. Marchant), isparra@ing.uchile.cl (I. Parra-Tsunekawa).
[1] Tel.: +56 2 978 4207; fax: +56 2 695 3881.

0921-8890/$ – see front matter © 2009 Elsevier B.V. All rights reserved.
doi:10.1016/j.robot.2009.03.011

A preliminary version of this work was presented in the RoboCup Symposium 2008. This extended version includes an improved fall's damage model (in each joint the radial torque was added to the model), a much more detailed evaluation and analysis of the proposed methodology (design examples using data obtained from human-activity videos and motion capture devices, more detailed experiments, and deeper analysis of pairs of fall sequences), and testing of the designed fall sequences in reality using the UCH H1 humanoid robot. In these tests a fast speed camera was employed to analyze the fall sequences.

This paper is organized as follows: In Section 2, some related work about human's fall is presented. The analysis of these studies suggests some guidelines for the management of falls in robots. The here-proposed methodology for the design of fall sequences that minimize the robot damage is described in Section 3. In Section 4, the presented methodology is used, as a case study, in the design process of fall sequences for simulated Nao humanoid robots, and validated in reality using the UCH H1 humanoid robot. Finally, in Section 5 some conclusions of this work are given.

2. Related work

Uncontrolled falls in biped humanoid robots have been largely ignored except for some very interesting works such as [5–7]. In general, falls are characterized by violent impacts that quickly dissipate and transfer important amounts of kinetic energy through joints, bones, and tissues. In this section, we will review some of the existing literature on human's falls, which can give us some insights on how to manage falls in robots. We will review several of the approaches to study falls in humans: what has been reported in medical literature, the studies done by researchers in biomechanics, the techniques developed in martial arts, and the results developed by the animation industry.

2.1. Medical studies

In [8] a fall is defined as "an unintentional event that results in a person's coming to rest on the ground or on another lower level". Falls are in general the result of the convergence of several intrinsic (muscle weakness, visual deficit, poor balance, gait defects, etc.), pharmacological (walking under the influence of alcohol, being under strong medication, etc.), environmental (uneven terrain, poor lighting conditions), and behavioral related factors (daily tasks, sports, violence, etc.) [9–11]. The rapid transmission of forces through the body that follow an impact against a surface causes injuries according to the magnitude and direction of the forces, the energy-absorbing characteristics of the surfaces that receive the impact, and the capacity of the tissues to absorb damage [10]. Fall prevention in humans has focused on balance and gait impairments, which are mainly affected by the interaction of the sensory (ability to determine whether the center of gravity of the body is within the support of the body or not), neuromuscular (transmission speed of the nervous impulses) and musculoskeletal systems (the available muscular force determine the range of possible movements), and their integration by the central nervous system (Parkinson's disease).

In general, falls from a standing height produce forces that are one order of magnitude greater than those necessary to break any bone of an elderly woman [10]. However, approximately no more than 10% of falls in older people cause fractures [9,10]. The most common examples of serious injuries, besides tissue and organ damage, are hip and wrist fractures [10]. This is a clear indicator that people constantly use fall-managing strategies that help to reduce injury-producing falls. Wrist injuries are also interesting because they indicate an active intent of people to stop their falls using limbs to shift the impact to less important organs or bones as the hands and the hips.

2.2. Biomechanical approach

Even though medical literature has been studying falls for several decades, the needs posed by high efficiency sports and the possibilities created by technological advances such as motion capture equipments has spawned new approaches to the science of human movement, also called biomechanics. This has made possible to understand human dynamics with greater detail and to generate more precise mathematical models of this biological machine:

(i) The musculoskeletal system is now modeled as a combination of something that exerts the force, a spring, and a damping system [12,13].
(ii) Machine learning approaches have been used to classify movements in order to understand their relationships, and to prove the existence of clusters of movement patterns [14].
(iii) It has been possible to determine the role of the center of mass of the body in all types of movements, i.e. rock climbing [15].
(iv) Another important aspect are interactions with external objects, where, for example, it has been possible to determine that people require several minutes to adjust their movements to changing asymmetrical loads [16,17], or how vision and limbs coordinate to follow and to manipulate balls while juggling [18].
(v) Control of synchronization between many people exhibiting rhythmic movements under some conditions has been proven to be independent from force control [19].

Of special interest, from the point of view of studying falls, are studies of people displaying fast interactions with the ground or objects. Of special interest is the study of Gittoes et al. [20], which proves that soft tissue strongly contributed to reduce loading when landing on the ground. Other studies of voluntary fast transitions show that it is possible to generate complex activation patterns that allow control sudden movements with an amazing degree of control [21–24].

2.3. Martial arts

In the previous paragraphs we have pointed out the biological aspects of falling. But, is it possible to control a fall in order to minimize damage? Is it possible to modify a fall in order to achieve some dynamic objective such as continuing running as fast as possible? These questions have been answered long ago by martial arts (see [25]). Out of these, Judo and Taekwondo, are perfect examples. Both disciplines teach how to fall from different positions: forward, backward, and sideways. All these techniques are extremely effective in the sense that produce a sequence of movements that vary the geometry of the human body in order to lower the force of the impacts, and spread the kinetic energy transfer through a wider contact area, a longer lapse of time, and limb movements. Moreover, some of these techniques are designed to allow the fighter to move away from the attacker and prepare himself to continue the combat by quickly recovering an upright stance.

2.4. Human dynamics simulation

The constant pressure of the computer animation market for more realistic special effects has spurred a lot of research in this topic in the last decades [26–28]. This research has even tackled problems not studied by other disciplines, such as the reproduction of destructive movements that are impossible to study in humans due to their nature [29,30]. Given that the tools created by this industry are completely located in simulated environments, many of them naturally produce very realistic falls with physically plausible kinematics and dynamical interactions.

2.5. Summary

In general, human falls are characterized by unexpected or expected impacts that affect the whole body. Overall, a fall should not be analyzed as a very local impact. On the contrary, its forces propagate along the entire body and help to distribute and dissipate its effects. In general, falls can be classified into three cases according to the degree of awareness of the person falling:

(i) The person is not aware of the fall and only passive elements of the body help to absorb the impacts. Given that every fall has a great potential for causing important body damage, there is strong evidence that the very nature of human joints, modeled with springs and dampers, and soft tissue passively contribute to ameliorate the effects of falls. In addition, medical literature reports that external padding may also help to diminish the effects of the falls.
(ii) The person detects when a fall is initiated and responds accordingly. This explains, for example, why wrist fractures are common: limbs are commonly used to change the impact points in order to redistribute the impact zones along the different surfaces of the body and over time.
(iii) As done in martial arts, if the person can predict a fall, then he/she can take control of the fall and change it into a fluid movement that helps to quickly recover the desired behavior. This is one step further into distributing the fall into different and wider surfaces of the body and over time, aiming towards diminishing or even eliminating fall damage.

When falls are considered from the point of view of robots, things change. For example, medical literature does not talk about joint damage but of bone fractures. In robots it is more plausible that the opposite is more important: it is always possible to build very strong limbs, while the motors in the joints are the ones that suffer damage during impacts. In this sense there has been work done that points out the problems that need to be solved in order to map human movement into robot movement [31].

In general, the study of human falls suggests that for robots it is important to:

(i) Design a body that passively helps as much as possible to walk and to fall. A body that uses joint models with springs and dampers as movable parts that act like soft tissue, and padding specially designed to protect important, frail, and/or expensive parts.
(ii) Detect a fall as soon as possible to trigger fall-related movements that allows reducing the fall damage.
(iii) If possible, predict falls and redesign normal moves in order to lower the probability of a fall, or to simply control a fall in order to eliminate it as much as possible or to reduce the damage.

This work is directly related with the design of fall-related movements that allows reducing the fall damage, and therefore connected to the second and third points.

3. A Methodology for designing fall sequences that minimize robot damage

3.1. Modeling

Let us consider a humanoid robot with n rotational articulations/joints q_i. Each articulation is composed by a DC motor, a gearbox and mechanical elements that fix these components (e.g. an articulation built up using a standard servomotor). In this model each articulation can rotate in a given angular operational range:

$$\theta_i^{\min} \le \theta_i \le \theta_i^{\max}; \quad i = 1, \dots, n. \tag{1}$$

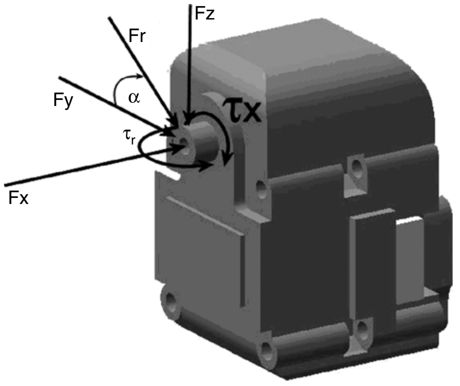

Fig. 1. External forces and torques that can damage an articulation, illustrated for the case of a Dynamixel DX117 motor.

The dynamics of each joint i can be characterized in terms of the forces and torques applied in the different axes. Due to the symmetry of the joints, only the axial and radial forces need to be considered. The axial force $F_a = F_x$ and the magnitude of the radial force $F_r = \sqrt{F_y^2 + F_z^2}$ (see Fig. 1) are external forces that can damage the articulation due to impacts produced during a fall. The rotational torque $\tau_{rot} = \tau_x$ is an external torque applied in the direction of rotation of the joint, while the radial torque $\tau_{rad} = \tau_r$ is the torque produced by the radial force. These forces and torques can be produced directly by the fall impacts or be transmitted by the robot body to the articulation. In the short period of time after an impact, a joint can be damaged if the linear or angular impulses (i.e. the integral of each external forces or torques over the time period) surpass a given magnitude that depends on the physical properties of the articulation (motor characteristics, gear material, etc.). Let us define J_{fa}, J_{fr}, J_{rot} and J_{rad} as the impulses produced by the axial force, radial force, rotational torque, and radial torque respectively. The damage can be avoided if the following relations hold:

$$\begin{aligned} &J_{i,fa} \le J_{i,fa}^{\max}; \qquad J_{i,fr} \le J_{i,fr}^{\max}; \qquad J_{i,rot} \le J_{i,rot}^{\max}; \\ &J_{i,rad} \le J_{i,rad}^{\max}; \qquad i = 1, \dots, n \end{aligned} \tag{2}$$

with $J_{i,fa}^{\max}, J_{i,fr}^{\max}, J_{i,rot}^{\max}, J_{i,rad}^{\max}$ threshold values that depends on the physical properties of the joint.

In addition to the joints' damage, the robot body (mainly frames) can be damaged if the intensity of the fall surpasses a given threshold. Therefore, we need a global measure of the fall intensity. In the biomechanics literature and in studies about falls in humans the impact velocity v_{imp} is used as a measure of the fall intensity. From the physics point of view, in rigid body collisions the damage is produced by the change of momentum of the colliding objects. Given that in our case collisions are produced between the robot and the ground, which has a much larger mass than the robot, we can assume that the impact velocity is an adequate measure of the fall impact. Hence, to avoid robot body damage, the following should hold:

$$v_{imp} \le v_{imp}^{\max} \tag{3}$$

with $v_{imp}^{\max}$ the maximal impact velocity that do not produce damage in the robot.

Naturally, (2) and (3) are related because the change of the total momentum, which depends on the impact velocity, is equal to the total impulse. This total impulse is then propagated through the robot body, producing local impulses in the joints. In this sense, we have mentioned both measures because in the simulation environment, the impulses over each joint during a fall can be easily obtained, but in real robots, these measures are difficult to obtain. However, with the use of a high speed camera we can track selected points in the robot, and their velocities can be estimated, then we can test falls designed in a simulation environment using real robots.

An important additional requirement to avoid the robot damage is that valuable body parts (CPU, cameras, etc.) should be protected. We assume that these parts will be protected if they do not touch the ground or if they touch it at a low speed. Let us consider K valuable body parts, then the following constraints should hold for each of them:

$$p_z^k > 0 \vee v_z^k \le v_{k,z}^{\max}; \quad k = 1, \dots, K \tag{4}$$

with p_z^k and v_z^k the vertical position and speed of each valuable part, respectively.

Let us define the joints' positions during the whole fall period as $\Theta_{T_{Fall}} = \{\Theta(t)\}_{t=0,\dots,T_{Fall}} \in \Theta^*$, with $\Theta(t)$ a vector containing the joints' positions at time step t, T_{Fall} the fall period, and Θ^* the domain of all possible joint configurations over different periods of time. The process of designing a fall sequence is modeled as a search for the $\Theta_{T_{Fall}}$ that minimizes the damage produced by the fall in robot's joints, frames and valuable parts. From (1)–(4), the general expression that model the proposed optimization problem, for a given $\Theta_{T_{Fall}}$, is given by:

$$\min_{\Theta_{T_{Fall}} \in \Theta^*} f(\Theta_{T_{Fall}}, J_{i,fa}, J_{i,fr}, J_{i,rot}, J_{i,radial}, v_{imp})$$

subject to

$$\begin{aligned} & J_{i,fa} \le J_{i,fa}^{\max}; \qquad J_{i,fr} \le J_{i,fr}^{\max}; \qquad J_{i,rot} \le J_{i,rot}^{\max}; \\ & J_{i,rad} \le J_{i,rad}^{\max}; \quad i = 1, \dots, n \\ & p_z^k(t) > 0 \vee v_z^k(t) \le v_{k,z}^{\max}; \quad k = 1, \dots, K;\ t = 0, \dots, T_{Fall} \\ & \theta_i^{\min} \le \theta_i(t) \le \theta_i^{\max}; \quad i = 1, \dots, n;\ t = 0, \dots, T_{Fall}. \end{aligned} \tag{5}$$

In this work, a particular objective function to use with the simulation environment is defined as:

$$\min_{\Theta_{T_{Fall}} \in \Theta^*} f(\Theta_{T_{Fall}}, J_{i,fa}, J_{i,fr}, J_{i,rot}, J_{i,radial}) = \sum_{j=1}^{4} \alpha_j \left(\frac{\sum_{i=1}^{n} \beta_i \cdot J_{i,j}}{n} + \mu \cdot \max_{i=1\dots n} (J_{i,j})^{\gamma} \right) \tag{6}$$

with α_j and β_j weight factors that depends on the resistance of each axis and on the importance of each joint (e.g. the neck joint is far more important than a finger joint for a human) respectively, μ a weight factor of the global maximal impact measure over all joints, γ a constant that allow to control how a higher maximal increases the value of the objective function, and $J_{i,1} = J_{i,fa}, J_{i,2} = J_{i,fr}, J_{i,3} = J_{i,rot}, J_{i,4} = J_{i,rad}$; $i = 1, \dots, n$. It should be noted that in (6), the force and torque impulses should be measured in the short period of time after an impact. On the other hand, velocity terms have not been considered in this objective function, due to the redundancy of this measure respect of the impulses. Velocity will be considered just when we will analyze a fall in a real robot.

3.2. Proposed methodology

As already explained, the process of designing a fall sequence consists on searching for a $\Theta_{T_{Fall}}$ that minimizes an expression that quantifies the damage (Eq. (6)). However, to implement directly this search process is highly complex because:

(i) when working directly with real robots a large amount of experiments is required, which would eventually damage the robots,

(ii) it requires measuring in each joint two linear and two rotational impulse values, as well as the impact velocity, in real-time (at a rate of few milliseconds), and

(iii) the high-dimensionality of the parameter space; the search process requires the determination of the position of each joint during the whole fall period.

The first two problems can be overcome if a realistic simulator is employed for the analysis and design of the fall sequences. Using this computational tool, robot damage due to extensive experiments is avoided. In addition, if the simulator is realistic enough (see for example [32,33]), all physical quantities that need to be known for evaluating (6) can be easily determined. The high dimensionality of the parameter space is the hardest problem to be tackled. As a suboptimal design strategy, we propose a human-based design procedure consisting on iteratively applying the following consecutive steps: *synthesis of fall sequences* using a simulation tool, and *quantitative analysis* of the obtained sequences using Eq. (6). The proposed procedure consists of the following main components:

(i) *Fall Initialization*: The seeds of the design process, i.e. initial values for the joints' positions during the whole fall period, are examples of human falls, obtained either from standard videos of falls (e.g. martial arts or human sports) or from data acquired using motion capture equipments (e.g. exoskeletons). In this step, just some general concepts of a "good" falling movement are used: bend knees to lower the center of mass, protect important parts keeping them away of the ground or using robust parts to cover them during the fall. Due to the natural difference between human's bodies and robot's bodies, the human inspiration just helps us to have a general starting point on the design of a good fall.

(ii) *Fall Evaluation*: The second step consists on executing the current fall to evaluate the objective function, and to obtain the maximal impulses over the joints during the fall. An interactive tool is employed by a human operator for the synthesis of fall sequences (see example in Fig. 2). For each frame of the sequence, the designer set up all joints' positions and tests the current fall. After the fall is finalized, the objective function given by (6) is evaluated, and all the maximal impulses over the joints can be retrieved.

(iii) *Fall Re-Design*: The joints with maximal impulses indicate to the human operator what should be corrected in the fall. The human operator changes the position of the joints to reduce the impact over the joints with maximal impulses. In addition, the human operator has to move the joints with lower impulse values allowing them to dissipate part of the energy initially dissipated in the joints with high impulse values. The restrictions over the important and sensible parts of the robot (e.g. head) are reviewed in each step of this manual interaction process, to ensure that they are not touching the ground during the fall.

The steps (ii) and (iii) are repeated iteratively until the objective function gives acceptable low values, and the procedure ensures that all maximal impulses are controlled and all restrictions are accomplished.

It is important to note that the proposed human-based search strategy can be automated using any numeric search procedure such as GA (Genetic Algorithms) or PSO (Particle Swarm Optimization). However, due to the high complexity of the solution space, added to the fact that each experiment (fall sequence execution) is a time consuming task with current simulation tools, we are still not using those approaches.

In the next section we will describe how the proposed strategy has been used in the design of falls sequences for Nao robots in the simulated environment of Webots.

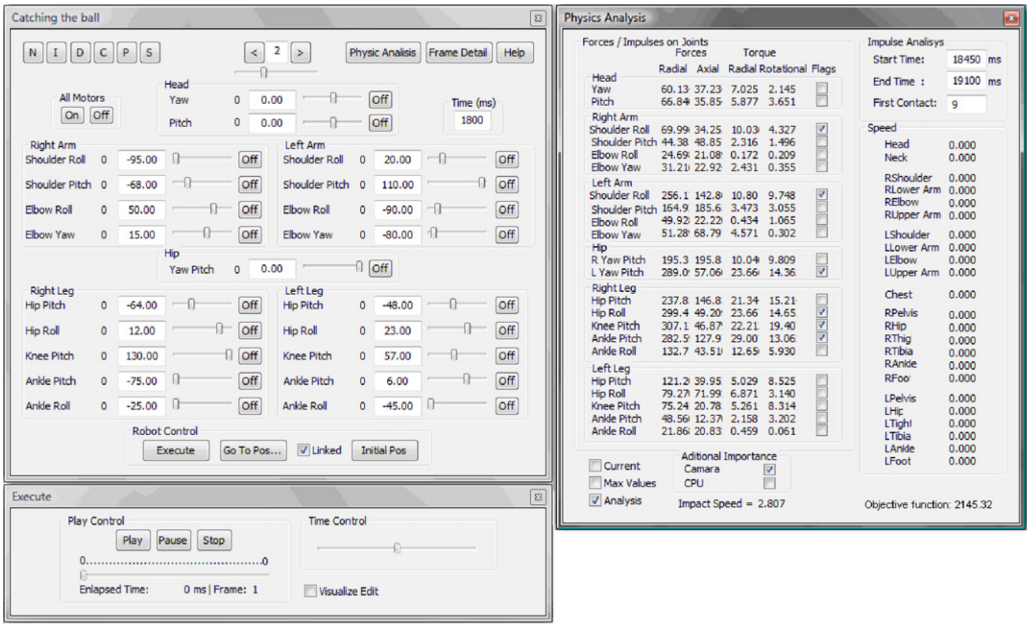

Frame: 2

Time (ms): 1800

Head			
Yaw	0	0.00	Off
Pitch	0	0.00	Off

Right Arm				Left Arm			
Shoulder Roll	0	-95.00	Off	Shoulder Roll	0	20.00	Off
Shoulder Pitch	0	-68.00	Off	Shoulder Pitch	0	110.00	Off
Elbow Roll	0	50.00	Off	Elbow Roll	0	-90.00	Off
Elbow Yaw	0	15.00	Off	Elbow Yaw	0	-80.00	Off

Hip			
Yaw Pitch	0	0.00	Off

Right Leg				Left Leg			
Hip Pitch	0	-64.00	Off	Hip Pitch	0	-48.00	Off
Hip Roll	0	12.00	Off	Hip Roll	0	23.00	Off
Knee Pitch	0	130.00	Off	Knee Pitch	0	57.00	Off
Ankle Pitch	0	-75.00	Off	Ankle Pitch	0	6.00	Off
Ankle Roll	0	-25.00	Off	Ankle Roll	0	-45.00	Off

☑ Linked

0...0

Enlapsed Time: 0 ms | Frame: 1

☐ Visualize Edit

Forces / Impulses on Joints

	Forces		Torque		
	Radial	Axial	Radial	Rotational	Flags
Head					
Yaw	60.13	37.23	7.025	2.145	☐
Pitch	66.84	35.85	5.877	3.651	☐
Right Arm					
Shoulder Roll	69.99	34.25	10.03	4.327	☑
Shoulder Pitch	44.38	48.85	2.316	1.496	☐
Elbow Roll	24.69	21.08	0.172	0.209	☐
Elbow Yaw	31.21	22.92	2.431	0.355	☐
Left Arm					
Shoulder Roll	256.1	142.8	10.80	9.748	☑
Shoulder Pitch	164.9	185.6	3.473	3.055	☐
Elbow Roll	49.92	22.22	0.434	1.065	☐
Elbow Yaw	51.28	68.79	4.571	0.302	☐
Hip					
R Yaw Pitch	195.3	195.8	10.04	9.809	☐
L Yaw Pitch	289.0	57.06	23.66	14.36	☑
Right Leg					
Hip Pitch	237.8	146.8	21.34	15.21	☐
Hip Roll	299.4	49.20	23.66	14.65	☑
Knee Pitch	307.1	46.87	22.21	19.40	☑
Ankle Pitch	282.5	127.9	29.00	13.06	☑
Ankle Roll	132.7	43.51	12.65	5.930	☐
Left Leg					
Hip Pitch	121.2	39.95	5.029	8.525	☐
Hip Roll	79.27	71.99	6.871	3.140	☐
Knee Pitch	75.24	20.78	5.261	8.314	☐
Ankle Pitch	48.56	12.37	2.158	3.202	☐
Ankle Roll	21.86	20.83	0.459	0.061	☐

☐ Current
☐ Max Values
☑ Analysis

Aditional Importance
Camara ☑
CPU ☐

Impact Speed = 2.807

Impulse Analisys
Start Time: 18450 ms
End Time : 19100 ms
First Contact: 9

Speed	
Head	0.000
Neck	0.000
RShoulder	0.000
RLower Arm	0.000
RElbow	0.000
RUpper Arm	0.000
LShoulder	0.000
LLower Arm	0.000
LElbow	0.000
LUpper Arm	0.000
Chest	0.000
RPelvis	0.000
RHip	0.000
RThig	0.000
RTibia	0.000
RAnkle	0.000
RFoo	0.000
LPelvis	0.000
LHip	0.000
LTight	0.000
LTibia	0.000
LAnkle	0.000
LFoot	0.000

Objective function: 2145.32

Fig. 2. Image capture of the interactive tool used for the falls design.

Table 1
Nao's joint names and motion ranges.

Body part	Id	Joint name	Motion	Range (degrees)
Head	1	HeadYaw	Head joint twist (Z)	−120 to 120
	2	HeadPitch	Head joint front & back (Y)	−45 to 45
Left arm	7	LShoulderPitch	Left shoulder joint front & back (Y)	−120 to 120
	8	LShoulderRoll	Left shoulder joint right & left (Z)	0 to 95
	9	LElbowRoll	Left shoulder joint twist (X)	−120 to 120
	10	LElbowYaw	Left elbow joint (Z)	0 to 90
Left leg	17	LHipYawPitch	Left hip joint twist ($Z45°$)	−90 to 0
	18	LHipPitch	Left hip joint front & back (Y)	−100 to 25
	19	LHipRoll	Left hip joint right and left (X)	−25 to 45
	20	LKneePitch	Left knee joint (Y)	0 to 130
	21	LAnklePitch	Left ankle joint front & back (Y)	−75 to 45
	22	LAnkleRoll	Left ankle joint right & left (X)	−45 to 25
Right leg	11	RHipYawPitch	Right hip joint twist ($Z45°$)	−90 to 0
	12	RHipPitch	Right hip joint front and back (Y)	−100 to 25
	13	RHipRoll	Right hip joint right & left (X)	−45 to 25
	14	RKneePitch	Right knee joint (Y)	0 to 130
	15	RAnklePitch	Right ankle joint front & back (Y)	−75 to 45
	16	RAnkleRoll	Right ankle right & left (X)	−25 to 45
Right arm	3	RShoulderPitch	Right shoulder joint front & back (Y)	−120 to 120
	4	RShoulderRoll	Right shoulder joint right & left (Z)	−95 to 0
	5	RElbowRoll	Right shoulder joint twist (X)	−120 to 120
	6	RElbowYaw	Right elbow joint (Z)	−90 to 0

4. Case study: Design of fall sequences for simulated Nao humanoid robots and validation in a real humanoid robot

4.1. Experimental tools and setup

To validate the proposed strategy, the problem of designing fall sequences for simulated Nao robots [34] was chosen. This robot was selected for the following reasons:

(i) it corresponds to an humanoid robot with 22 degrees of freedom (see Table 1 for details about the joints and their motion ranges), which represents a complex problem from the point of view of the design of fall sequences,
(ii) there is a realistic simulator available for this robot (Webots [32]) and
(iii) the simulator and the robot controller are URBI-compatible [35], which allows building an interactive interface for designing falls, without modifying the simulator or accessing to its source code.

The first step was to build a user interface that allows designing the falls, i.e. specifying the joints positions for the whole frame period ($\Theta(t)$; $t = 0, \ldots, T_{EndFall}$), and measuring the velocity and impulses values of the falls. This interface was built using URBI to interact with the robot, and using an ODE plug in to obtain forces and velocities form the simulator. Fig. 2 shows the appearance of the developed tool. It can be seen that:

(i) The main window contains the values of all joint positions for the current frame. These values can be modified by the designer (user).
(ii) The bottom window contains the commands for executing the fall, either continuously or in frame-to-frame mode.
(iii) The right window displays the values of the force and torque impulses, the impact velocity, and flags that indicate if any

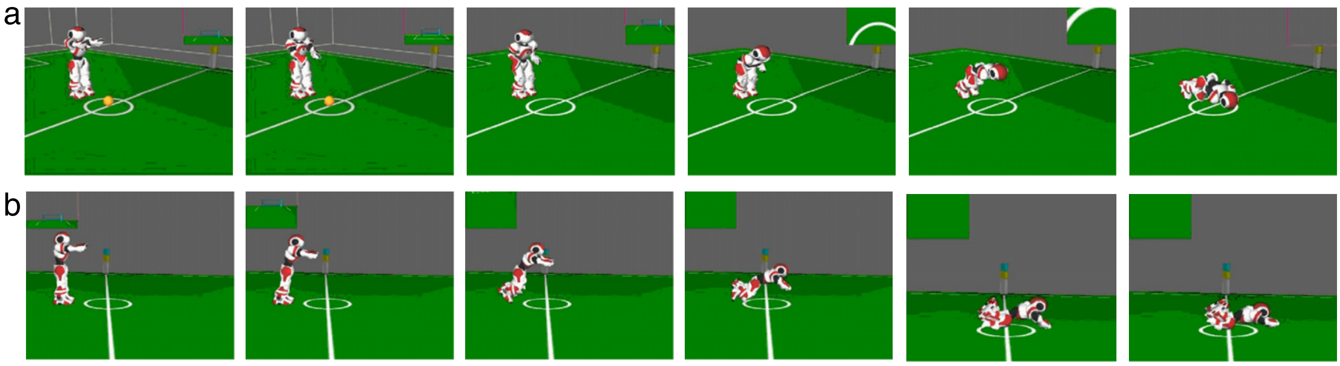

Fig. 3. Simulation sequences showing selected frames of the frontal falls under analysis. *FrontHead*: (a1)–(a6). *FrontLow*: (b1)–(b6).

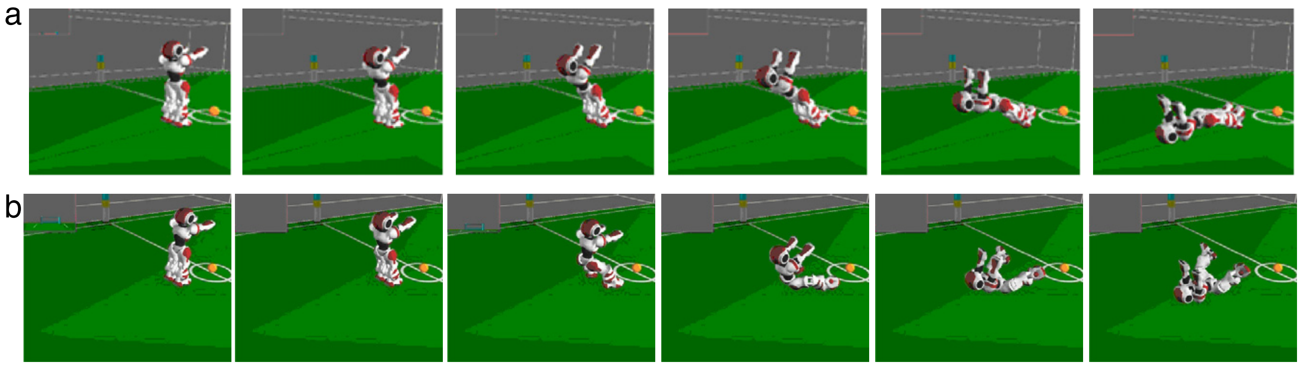

Fig. 4. Simulation sequences showing selected frames of the back falls under analysis. *BackHead*: (a1)–(a6). *BackLow*: (b1)–(b6).

Table 2
Impulses, maximal impulses and objective function over the joints.

BackHead fall	Joint ID																						Maximal impulses
Impulses	1	2	3	4	5	6	7	8	9	10	11	12	13	14	15	16	17	18	19	20	21	22	
Axial (Nm)	270.6	1.5	11.6	64.1	20.3	54.9	9.2	81.1	20.3	54.5	144.6	75.1	92.0	74.9	74.9	171.0	135.9	76.1	85.3	76.1	76.0	152.9	270.6
Radial (Nm)	368.4	437.5	139.9	74.7	46.8	23.9	179.4	89.9	46.4	23.9	142.8	192.0	187.8	192.5	209.9	168.8	139.9	178.2	178.0	176.1	189.4	157.9	437.5
Axial Tor. (Nms)	1.2	41.6	12.8	1.5	0.0	0.1	12.4	0.6	0.0	0.1	32.2	41.5	20.3	41.5	28.9	3.8	30.0	38.8	19.9	38.6	27.1	3.5	41.6
Radial Tor. (Nms)	101.4	0.1	13.5	6.0	0.3	3.3	15.2	5.2	0.3	3.3	33.2	21.1	44.7	21.1	12.6	17.3	33.8	20.2	41.6	20.2	11.6	16.2	101.4
Fitness value	3088.1																						
BackLow fall	Joint ID																						Maximal impulses
Impulses	1	2	3	4	5	6	7	8	9	10	11	12	13	14	15	16	17	18	19	20	21	22	
Axial (Nm)	26.5	0.5	0.1	19.4	11.7	36.4	0.1	19.4	11.7	36.4	200.3	67.1	61.1	67.3	50.4	21.5	198.7	71.1	58.7	67.4	50.5	21.6	200.3
Radial (Nm)	107.1	112.3	75.7	59.4	31.0	13.8	75.7	59.4	31.0	13.8	243.8	312.4	331.0	71.9	49.6	52.2	241.4	307.2	326.7	71.9	49.7	52.3	331.0
Axial Tor. (Nms)	0.1	7.6	10.5	0.2	0.0	0.1	10.5	0.2	0.0	0.1	24.1	20.0	4.1	6.3	4.1	0.5	23.8	19.8	4.1	6.3	4.1	0.5	24.1
Radial Tor. (Nms)	24.8	0.1	6.6	1.6	0.2	1.7	6.4	1.6	0.2	1.7	13.6	9.9	27.6	7.9	4.6	2.9	43.8	25.5	18.4	17.5	5.9	2.1	43.8
Fitness value	1575.2																						

of these values have surpassed their maximal thresholds. In addition, some flags indicate if valuable parts, camera and CPU in this case, touch the ground. The user employs this tool in the designing process, and he/she can see simultaneously the resulting fall sequence directly in the simulator main window (see examples of fall sequences obtained from the simulator main window in Figs. 3 and 5).

4.2. Design process of fall sequences

For the purpose of showing the potentiality of the proposed fall designing methodology, frontal and back "good" and "bad" fall sequences were designed; "good"/"bad" means low/high damage. The designed sequences are (see videos in [36]):

- *FrontHead*: Frontal fall sequence where the robot impacts the ground with its head. This is the typical frontal fall of a robot that do not detect it is falling. See Fig. 3(a1) to (a6).
- *FrontLow*: Frontal fall sequence where the robot folds its legs in order to lower its center of mass before the impact. The lowering of the center of mass allows reducing the impact velocity. See Fig. 3(b1) to (b6).
- *BackHead*: Back fall sequence where the robot impacts the ground with its head. This is the typical back fall of a robot that do not detect it is falling. See Fig. 4(a1) to (a6).

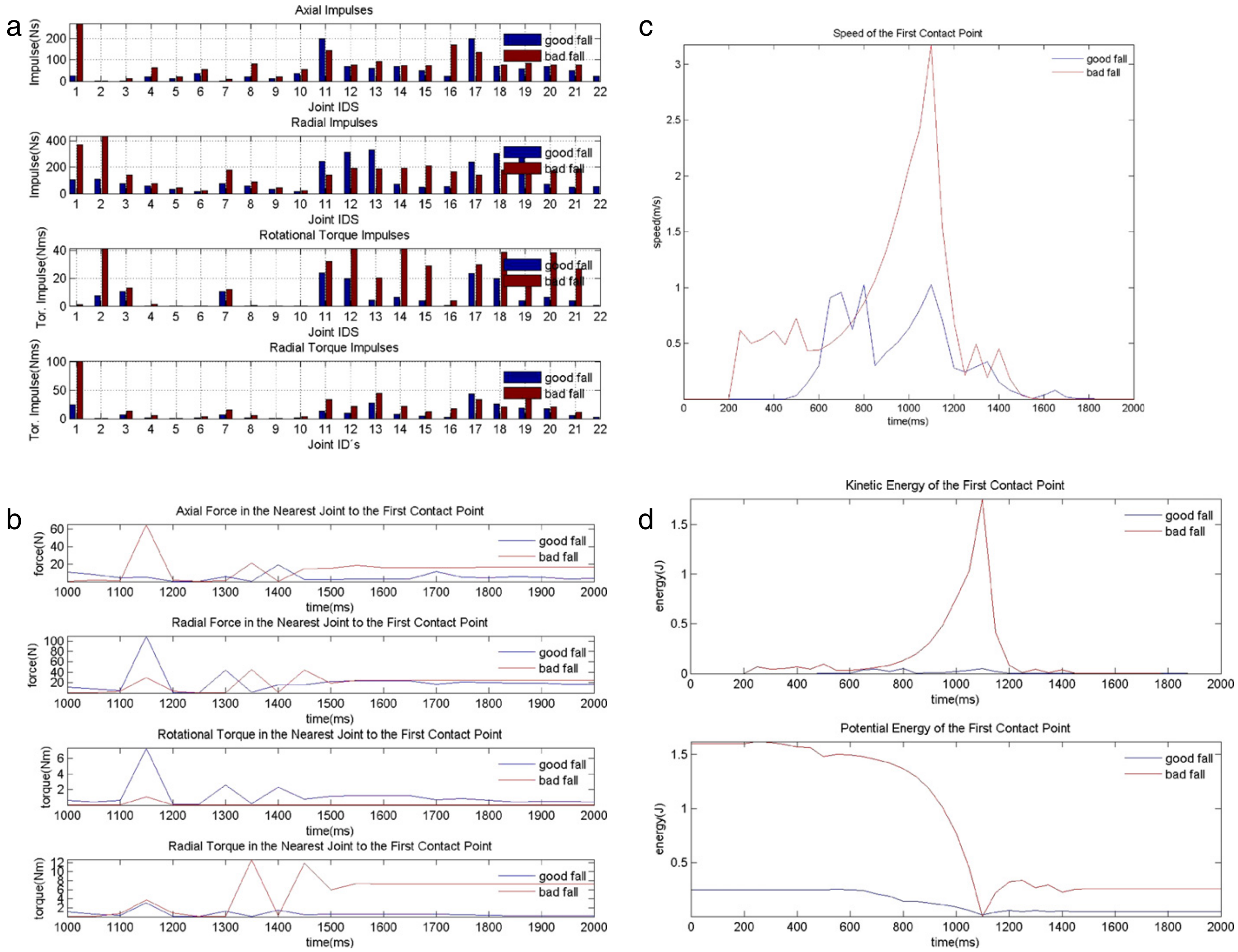

Fig. 5. *BackHead*/*BackLow* falls' indices in red/blue. In the first/second fall the head/right-hip impacts the ground after 1150 ms.

Table 3
Impulses, maximal impulses and objective function over the joints.

FrontHead fall	Joint ID																						Maximal impulses
Impulses	1	2	3	4	5	6	7	8	9	10	11	12	13	14	15	16	17	18	19	20	21	22	
Axial (Nm)	155.1	233.5	0.1	37.7	10.5	25.1	0.1	37.9	10.3	24.8	77.2	49.2	73.4	49.2	49.1	145.7	80.9	50.4	68.8	50.5	50.5	140.3	233.5
Radial (Nm)	263.7	217.0	71.6	44.4	29.4	24.8	71.7	44.1	29.6	25.0	87.3	106.9	105.3	146.7	171.7	110.9	89.4	108.1	109.2	143.5	167.7	113.3	263.7
Axial Tor. (Nms)	0.0	10.5	6.8	1.0	0.3	0.1	6.8	0.7	0.3	0.2	21.3	27.2	11.4	26.9	16.9	2.3	21.1	26.6	11.8	26.2	16.8	2.1	27.2
Radial Tor. (Nms)	62.1	10.5	7.4	2.2	0.5	2.6	7.0	2.2	0.0	1.3	23.3	12.2	39.4	12.2	6.6	20.6	12.6	12.5	39.1	12.5	6.7	20.7	62.1
Fitness value	1679.2																						
FrontLow fall	Joint ID																						Maximal impulses
Impulses	1	2	3	4	5	6	7	8	9	10	11	12	13	14	15	16	17	18	19	20	21	22	
Axial (Nm)	17.4	13.4	16.6	91.5	88.6	89.5	26.5	69.4	58.4	43.9	43.8	29.6	130.9	30.9	23.1	17.9	57.2	37.4	161.5	27.1	17.1	28.1	161.5
Radial (Nm)	79.2	68.3	147.7	108.5	100.5	102.8	100.0	59.6	42.6	61.7	178.6	164.7	54.1	98.8	62.6	42.2	196.1	191.9	75.2	84.3	73.6	40.3	196.1
Axial Tor. (Nms)	1.3	3.9	25.5	4.6	5.4	6.1	17.5	3.4	2.6	4.1	6.0	7.1	2.7	7.2	4.7	0.3	3.3	6.6	1.9	6.9	4.1	0.3	25.5
Radial Tor. (Nms)	14.8	1.3	7.4	11.7	9.5	18.1	10.0	10.3	5.1	9.6	22.7	4.2	9.8	3.5	2.4	0.9	12.6	2.0	9.9	3.6	1.9	0.9	22.7
Fitness value	887.3																						

- *BackLow*: Back fall sequence where the robot separates and folds its legs in order to lower its center of mass before the impact. This action reduces the impact velocity. See Fig. 4(b1) to (b6).

It is important to stress that the process of finding "good" fall sequences is a very difficult task, due to the high dimensionality of the search space. The first step of the proposed methodology described in Section 3.2, says that we need use some basic human based behaviors as lower the center of mass and protect the important parts to find an initial fall. In our case the initial *FrontLow* and *BackLow* falls were designed by analyzing data generated by a motion capture exoskeleton (Gypsy-5 from Animazoo [37]) and analyzing videos of martial arts. These initial falls were

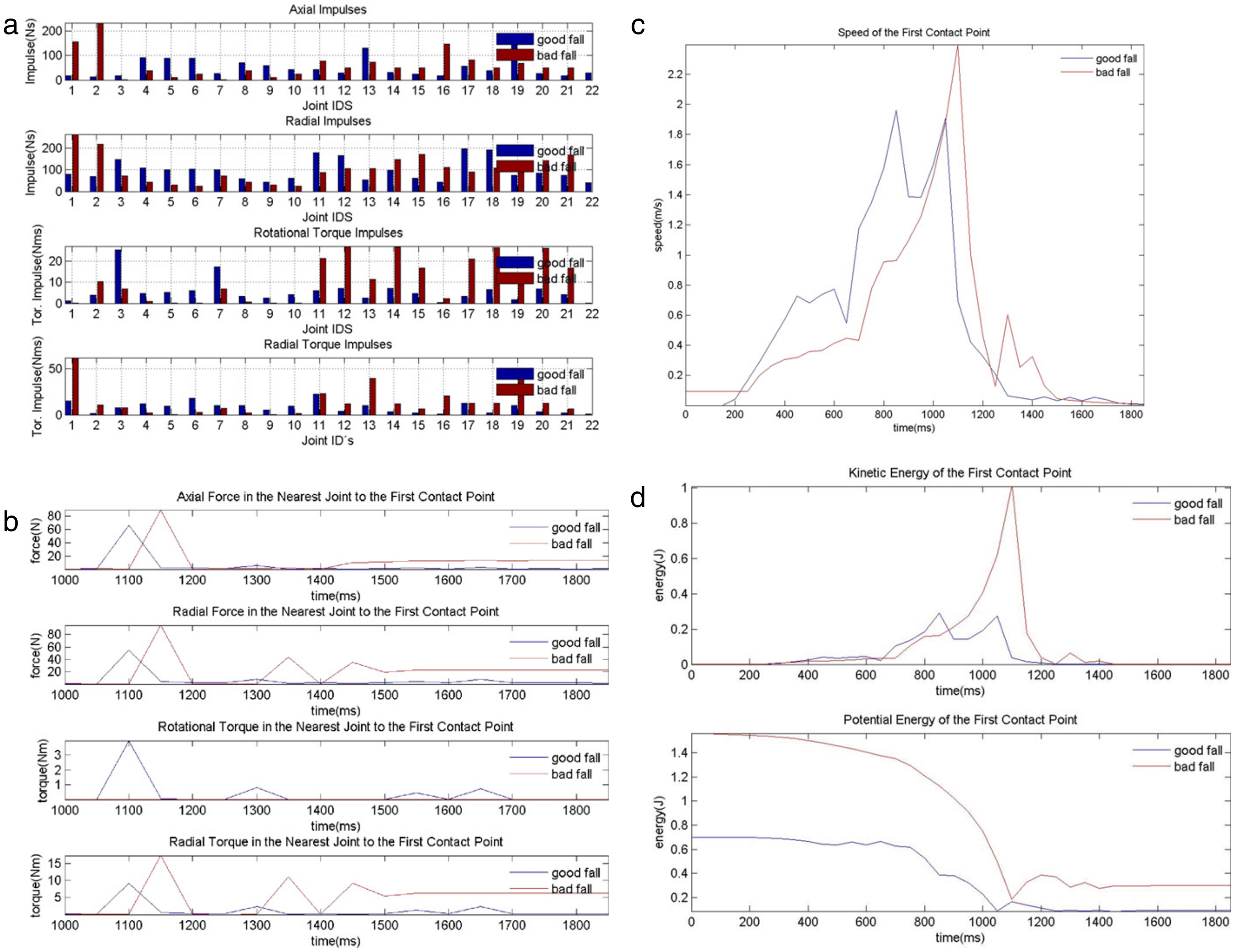

Fig. 6. *FrontHead*/*FrontLow* falls' indices in red/blue. In the first/second case the head/right-lower arm impacts the ground after 1150 ms/1100 ms.

iteratively improved following the steps (ii) and (iii) of the proposed methodology. Although the final results look like the original human inspirited falls, to obtain falls with low damage values that accomplish the proposed restrictions, it is necessary to make several iterations of the step (ii) and (iii) of the methodology (almost 5–10 iterations for each fall), to decrease progressively the maximal impulse values, while the objective function decreases until an acceptable value.

4.3. Analysis of the fall sequences

Figs. 5 and 6 show comparisons in terms of force and torque impulses in each joint, force and torque values in the nearest joint to the first contact point, and speed, potential energy and kinetics energy of the first contact point. Tables 2 and 3 resumes the impulses data, the maximal values, and the result of the objective function for each pair of compared falls. The joint IDs can be seen in Table 1. The parameters of the objective function (Eq. (6)) are:

- $\alpha_{axial} = \alpha_{radial} = 0.25$ (due to the used units, the magnitude of the impulses produced by the forces are 4 times the impulses produced by the torques)
- $$\alpha_{radial-torque} = \alpha_{axial-torque} = \mu = \beta_i = 1.0; \quad i = 1, \ldots, n$$
- $\gamma = 1.5$ (this value was adequate to penalize enough the maximal values of the impulses).

As it can be observed in Fig. 5 and Table 2, much larger maximal impulses are obtained in the *BackHead* fall sequence than in the *BackLow* fall sequence: 271 Ns vs. 200 Ns in the case of the axial force impulse, 437 Ns vs. 331 Ns in the case of the radial force impulse, 42 Nms vs. 24 Nms in the case of the rotational torque impulse, and 101 Nms vs. 49 Nms in the case of the radial torque impulse. In addition, in the case of the *BackHead*, fall maximal impulses are produced mainly in the head articulations (IDs 1 and 2), while in the *BackLow* fall, maximal impulses are produced in the right hip articulation (IDs 11–13) and in the left hip articulation (IDs 17–19), which are less vulnerable parts than the head. It can be also observed that in the *BackHead* fall, the axial force at the impact time is very high in the head (60 N), and that also a very high radial torque (12 Nm) is produced later on in the head. In the case of the *BackLow* fall the radial force and the rotational torque at the impact time are very high in the right hip, 100 N and 6.5 Nm, respectively. Regarding the speed, we can see that at the impact time, the speed of the contact point in the case of the *BackHead* fall (the head) is more than three times larger than in the case of the *BackLow* fall (right hip). Finally, if we analyze the magnitude of the kinetic and potential energy, we can observe that much larger values are observed in the case of the *BackHead* fall than in the case of the *BackLow* fall. Impact speed, kinetic energy and potential energy are

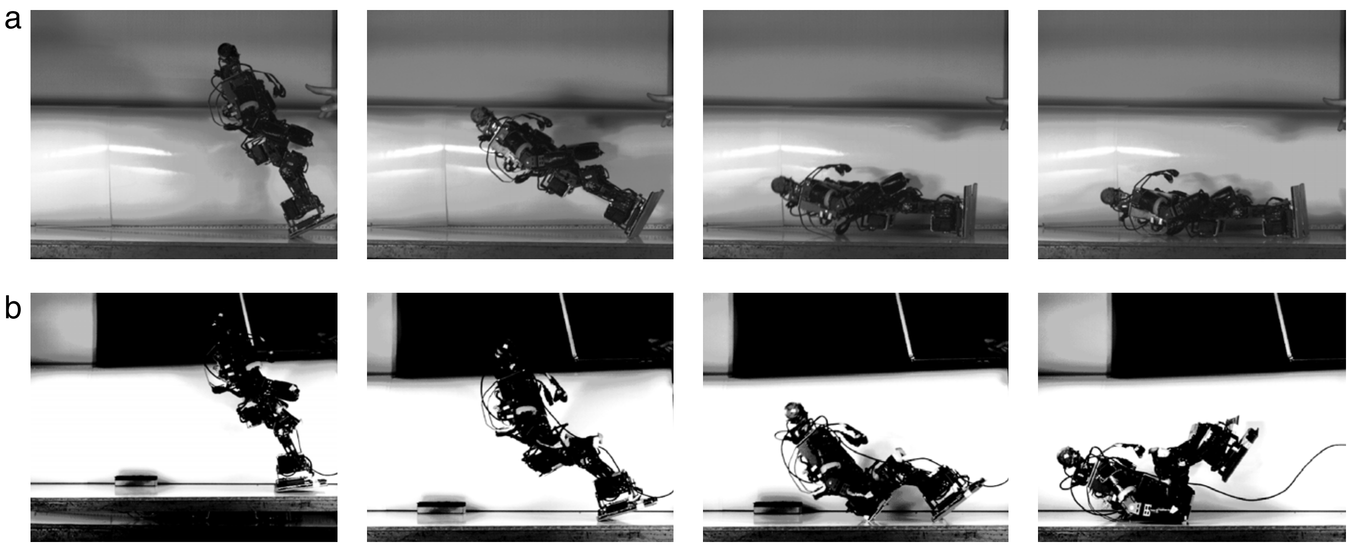

Fig. 7. Simulation sequences showing selected frames of the back falls under analysis. *BackHead*: (a1)–(a4). *BackLow*: (b1)–(b4).

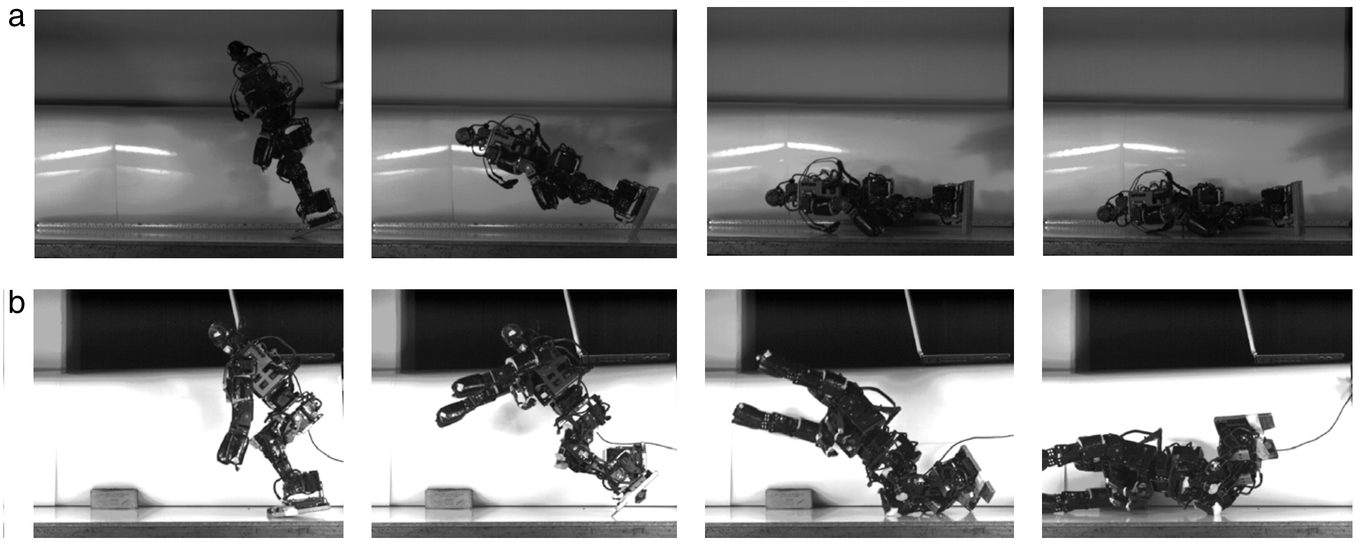

Fig. 8. Simulation sequences showing selected frames of the frontal falls under analysis. *FrontHead*: (a1)–(a4). *FrontLow*: (b1)–(b4).

global measures of the magnitude of the impact. The value of the objective function for the *BackHead* fall is two times larger than the *BackLow* fall, which shows that the employed objective function is a good indicator of the fall's quality.

Fig. 6 and Table 3 show indices of the *FrontHead* and *FrontLow* fall sequences. As in the former case, we observe that in all axes the maximal impulses obtained in the bad fall case are larger than the ones obtained in the good fall: 233 Ns vs. 161 Ns, 264 Ns vs. 196 Ns in, 27 Nms vs. 26 Nms, and 62 Nms vs. 23 Nms for the axial force impulse, radial force impulse, rotational torque impulse, and radial torque impulse, respectively. In addition higher impulse values are produced in a valuable articulation (the head) for the case of the bad fall sequence, while in the case of good fall sequence higher impulse values are produced in stronger articulations (hip and knee). The *FrontHead* fall shows very high radial force, axial force and radial torque values in the head articulations, 80 N in the first two cases and 57 Nm in the last case. The *FrontLow* fall shows relative high rotational torque values (3.8 Nm) in the hip. Regarding impact velocity, in the *FrontHead* fall is about 20% higher than in the *FrontLow* case. It is important to stress that in the first case the first contact point with the ground is in the head, while in the second case it is in the right lower arm. The magnitude of the kinetic energy at impact time is more than 3 times larger in the case of the *FrontHead* fall. The potential energy shows much higher values in the case of the *FrontHead* fall, during the whole falling period. Finally, the objective function is two times larger in the *FrontHead* fall case than in the *FrontLow* case.

4.4. Fall sequences validation in reality

To validate our methodology, the fall sequences were transferred to a real humanoid robot. Due to the current fragility of Nao robots, we could not use them in these experiments. Instead, we tested the fall sequences in a more robust humanoid robot, the UCH H1 robot (see description in [38]), which has a similar structure than Nao robots, but it has much stronger frames and joints.

In a real robot we cannot measure the force and torque impulses in the different articulations. However, the speed and acceleration of some body parts, which are related to the impulses, are good indicators of the fall sequences damage, and can be measured in reality. To carry out these measurements we used a fast speed camera [39], and we analyzed the falls using a video sequence

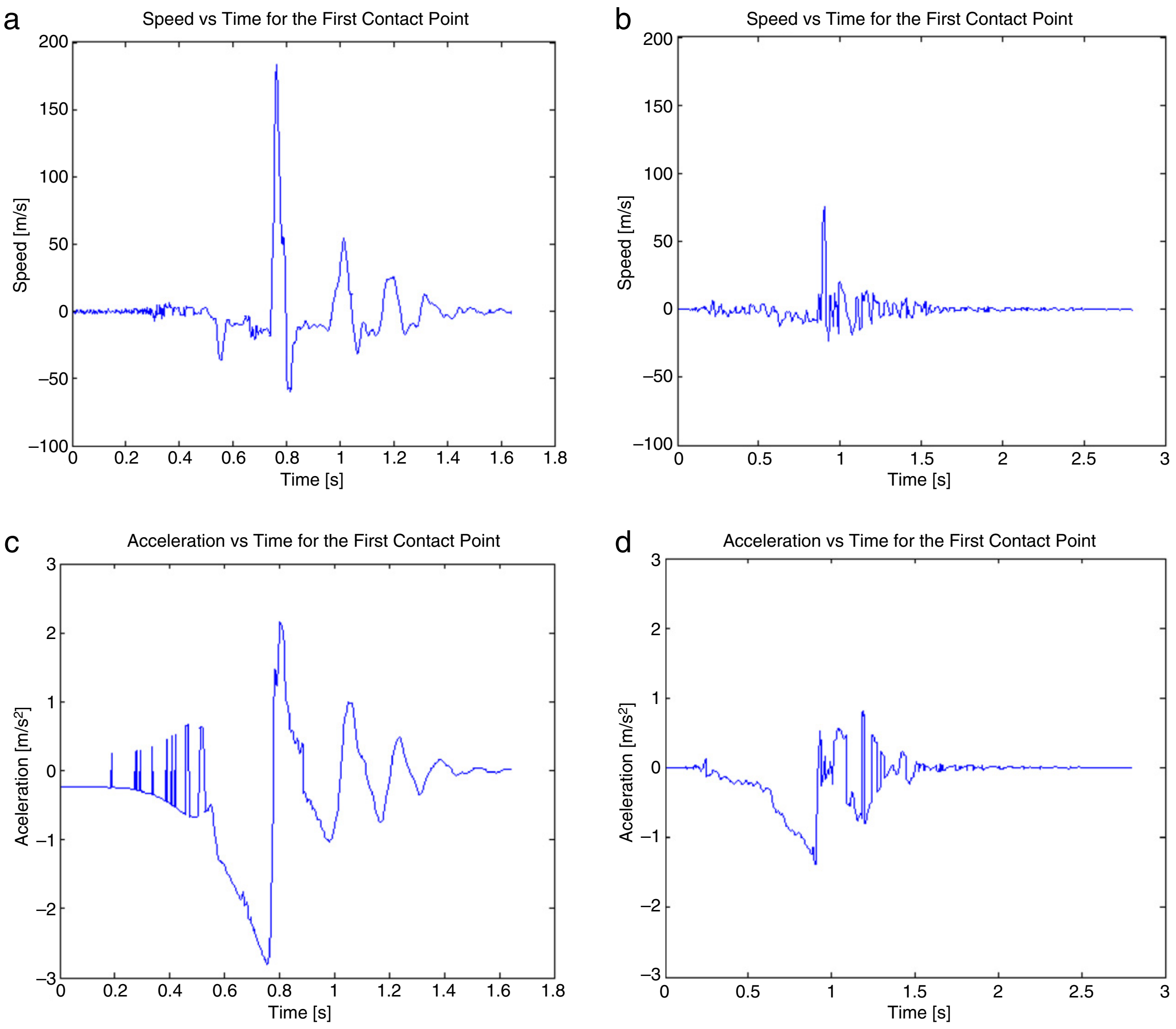

Fig. 9. *BackHead*/*BackLow*-fall's speed and acceleration of the first robot's contact-point. (a) and (c) correspond to *BackHead* fall, and (b) and (d) to *BackLow* fall.

taken at 500 fps, with a resolution of 1280 × 1024 pixels (see some selected frames in Figs. 7 and 8). Speed and acceleration of selected body parts were obtained by tracking these points in the video sequences.

Speed and acceleration graphs of the robot's first contact point, for all fall sequences under analysis are displayed in Figs. 9 and 10. It can be observed that much lower values of speed and acceleration are obtained in the cases of the designed *BackLow* and *FrontLow* fall sequences, and that therefore they produced much less damage in the robot than the *BackHead* and *FrontHead* fall sequences. While the *BackHead* and *FrontHead* have a maximal speed of 175 m/s, the *BackLow* and *FrontLow* falls have just 75 m/s as maximal speed. The module of the vertical acceleration impulse produced at the moment of the impact, is reduced from 5.0 m/s^2 to 2.2 m/s^2 if the *BackLow* fall is used instead of the *BackHead* fall. If we compare the *FrontHead* and *FrontLow* falls, the module of the acceleration impulse is reduced from 4.7 m/s^2 to 2.2 m/s^2. These measurements validate the results obtained in the simulation process.

Furthermore, we estimated the potential head damage (e.g. neck articulations) by measuring the derivative of the acceleration in the head at the impact time. The obtained values were 220 m/s^3 and 63.1 m/s^3 for the *BackHead* and *BackLow* falls, respectively, and 261 m/s^3 and 27.2 m/s^3 for the *FrontHead* and *FrontLow* fall, respectively. Again, the Fig. 4(a1) to (a4) and (b1) to (b4) show that much less damage is produced in the *BackLow* and*FrontLow* cases.

5. Conclusions

In this paper, a methodology for designing fall sequences that minimize the robot damage was presented. The methodology consists basically on to model the fall design process as a search procedure that looks for the joints' values that minimize the robot's damage. The search process is human-based, and it includes the use of a realistic simulator for the synthesis and analysis of the falls, and an interactive tool that allows the human designer to select fall sequence parameters (joints values, sequences extension, etc.), and to observe damage's indices that indicate the quality of the obtained sequence.

Experiments using a simulated humanoid robot, which were validated in a real humanoid robot, show that modeling falls after what is observed in humans greatly decreases the robot damage. Thus, longer fall sequences, with several contact points, and a lowering of the center of mass produce much less damage in the robot. In addition, fall sequences that protect valuable body parts, as the head, can also be designed using the proposed methodology.

As future work, we would like to:

(i) Use the designed fall sequences in real soccer games.
(ii) Automate the human-based search strategy using any numeric search procedure such as GA (Genetic Algorithms) or PSO (Particle Swarm Optimization).

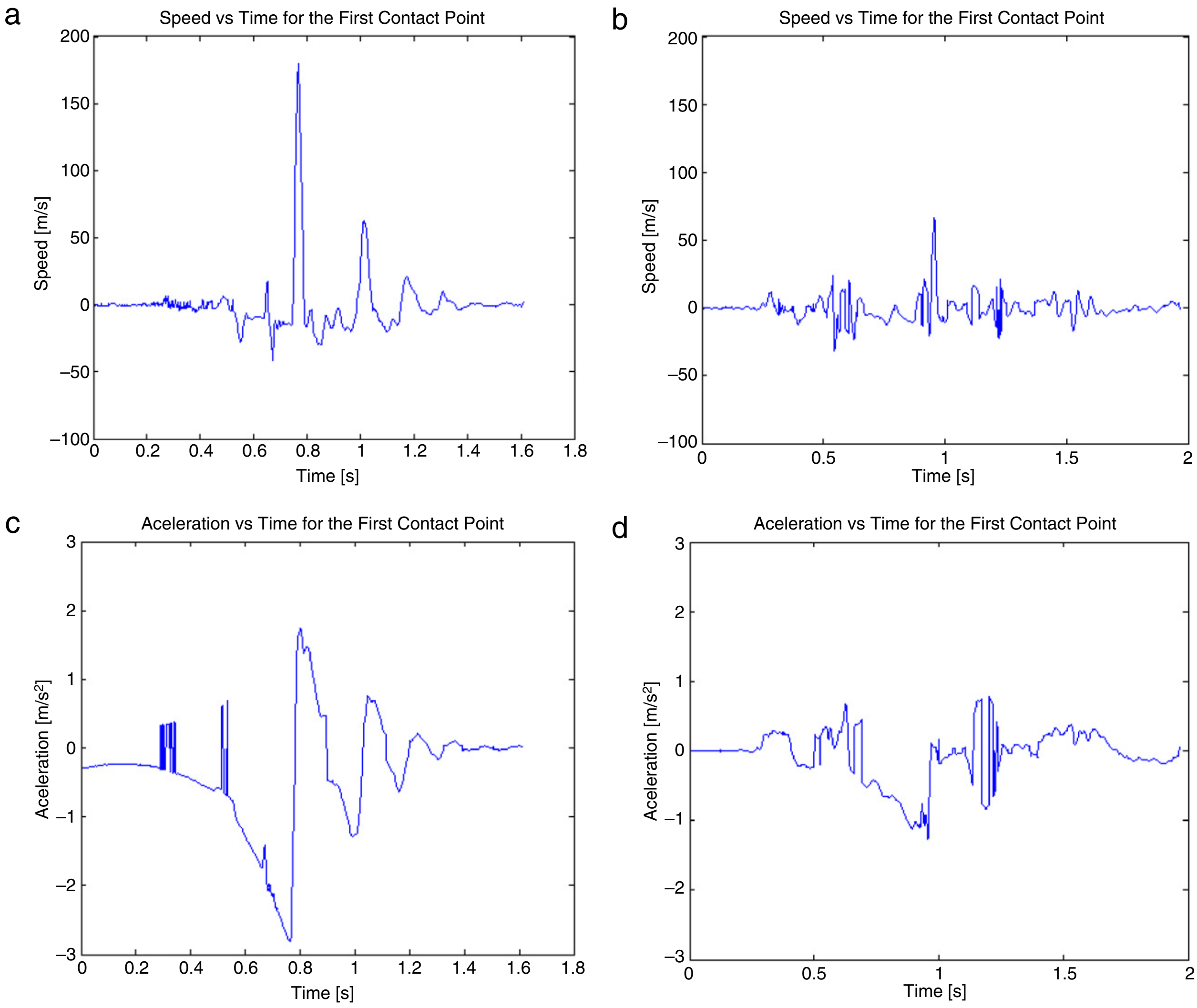

Fig. 10. *FrontHead*/*FrontLow*-fall's speed and acceleration of the first robot's contact-point. (a) and (c) correspond to the *FrontHead* fall, and (b) and (d) to *FrontLow* fall.

Acknowledgement

This research was partially funded by FONDECYT project 1090250, Chile. For their support we thank Professor Nicolas Mujica (Universidad de Chile), who facilitates us the use of the MOTION PRO X3 Camera, and Dr. Olivier Michel (Cyberbotics), who facilitates us the use of the Webots simulator.

References

[1] J. Baltes, S. McGrath, J. Anderson, The use of gyroscope feedback in the control of the walking gaits for a small humanoid robot, in: RoboCup 2004, in: Lecture Notes in Computer Science, vol. 3276, 2005, pp. 628–635.

[2] O. Höhn, J. Gacnik, W. Gerth, Detection and classification of posture instabilities of bipedal robots, in: Proc. of the 8th Int. Conf. on Climbing and Walking Robots and the Support Technologies for Mobile Machines-CLAWAR, 2005, pp. 409–416.

[3] M. Morisawa, S. Kajita, K. Harada, K. Fujiwara, K.K. Fumio Kanehiro, H. Hirukawa, Emergency stop algorithm for walking humanoid robots, in: Proc. 2005 IEEE/RSJ Int. Conf. on Intelligent Robots and Systems, 2005, pp. 2109–2115.

[4] R. Renner, S. Behnke, Instability detection and fall avoidance for a humanoid using attitude sensors and reflexes, in: Proc. 2006 IEEE/RSJ Int. Conf. on Intelligent Robots and Systems, 2006, pp. 2967–2973.

[5] K. Fujiwara, F. Kanehiro, S. Kajita, K. Kaneko, K. Yokoi, H. Hirukawa, UKEMI: Falling motion control to minimize damage to biped humanoid robot, in: Proc. 2002 IEEE/RSJ Int. Conference on Intelligent Robots and System, vol. 3, 2002, pp. 2521–2526.

[6] K. Fujiwara, F. Kanehiro, H. Saito, S. Kajita, K. Harada, H. Hirukawa, Falling motion control of a humanoid robot trained by virtual supplementary tests, in: Proc. 2004 IEEE Int. Conf. on Robotics and Automation, 2004, pp. 1077–1082.

[7] P.R. Pagilla, B. Yu, An experimental study of planar impact of a robot manipulator, IEEE/ASME Transactions on Mechatronics 9 (1) (2004) 123–128.

[8] Kellog international work group on the prevention of falls by the elderly, the prevention of falls in later life, Danish Medical Bulletin 34 (4) (1987) 1–24.

[9] M.B. King, Evaluating the older person who falls, in: J.C. Masdeu, L. Sudarsky, L. Wolfson (Eds.), Gait Disorders of Aging: Falls and Therapeutics Strategies, Lippincott-Raven Publishers, 1997.

[10] M.C. Nevitt, Falls in the elderly: Risk factors and prevention, in: J.C. Masdeu, L. Sudarsky, L. Wolfson (Eds.), Gait Disorders of Aging: Falls and Therapeutics Strategies, Lippincott-Raven Publishers, 1997.

[11] L.Z. Rubenstein, K.R. Josephson, Interventions to reduce the multifactorial risks for falling, in: J.C. Masdeu, L. Sudarsky, L. Wolfson (Eds.), Gait Disorders of Aging: Falls and Therapeutics Strategies, Lippincott-Raven Publishers, 1997.

[12] M. Nikanjam, K. Kursa, S. Lehman, L. Lattanza, E. Diao, Eand D. Rempel, Finger flexor motor control patterns during active flexion: an in vivo tendon force study, Human Movement Science 26 (2007) 1–10.

[13] M.H.E. Lussanet, J.B.J. Smeets, E. Brenner, Relative damping improves linear mass-spring models of goal-directed movements, Human Movement Science 21 (2002) 85–100.

[14] J. Perl, A neural network approach to movement pattern analysis, Human Movement Science 23 (2004) 605–620.

[15] F. Sibella, I. Frosio, F. Schena, N.A. Borghese, 3D analysis of the body center of mass in rock climbing, Human Movement Science 26 (2007) 851–852.

[16] J.D. Smith, P.E. Martin, Walking patterns change rapidly following asymmetrical lower extremity loading, Human Movement Science 26 (2007) 412–425.

[17] C. Teulier, Delignies, The nature of the transition between novice and skilled coordination during learning to swing, Human Movement Science 26 (2007) 376–392.

[18] R. Huys, A. Daffertshofer, P.J. Beek, Multiple time scales and subsystem embedding in the learning of juggling, Human Movement Science 23 (2004) 315–336.

[19] E.N. Rousanoglou, K.D. Boudolod, Rhythmic performance during a whole body movement: Dynamic analysis of force-time curves, Human Movement Science 25 (2006) 393–408.

[20] M.J. Gittoes, M.A. Brewin, D.G. Kerwin, Soft tissue contributions to impact forces simulated using a four-segment wobbling mass model of forefoot-heel landings, Human Movement Science 25 (2006) 775–787.
[21] H. Katsumata, A functional modulation for timing a movement: A coordinative structure in baseball hitting, Human Movement Science 26 (2007) 27–47.
[22] S.R. Caljouw, J. van der Kamp, Bi-phasic hitting with constraints on impact velocity and temporal precision, Human Movement Science 24 (2005) 206–217.
[23] H. Ertan, B. Kentel, S.T. Tumer, F. Korkusuz, Activation patterns in forearm muscles during archery shooting, Human Movement Science 22 (2003) 37–45.
[24] P.N. Loseby, J.P. Piek, N.C. Barret, The influence of speed and force on bimanual finger tapping patterns, Human Movement Science 20 (2001) 531–547.
[25] B.E. Groen, V. Weerdesteyn, J. Duysens, Martial arts fall techniques decrease the impact forces at the hip during sideways falling, Journal of Biomechanics 40 (2007) 458–462.
[26] E. Pavey, Ready for their close-ups: Breathing life into digitally animated faces, IEEE Spectrum Magazine 42–47 (April) (2007).
[27] Y. Abe, J. Popovic, Interactive animation of dynamic manipulation, in: Proc. of the Eurographics/ ACM SIGGRAPH Symposium on Computer Animation, Vienna, Austria, 2006.
[28] C.K. Liu, A. Hertzmann, Z. Popovic, Learning physics-based motion style with nonlinear inverse optimization, ACM Transactions on Graphics 24 (3) (2005) 1071–1081.
[29] T. Reil, P. Husbands, Evolution of central pattern generators for bipedal walking in a real-time physics environment, IEEE Transactions on Evolutionary Computation 6 (2) (2002) 159–168.
[30] G.S. Hornby, J.B. Pollack, Creating high-level components with a generative representation for body-brain evolution, Artificial Life 8 (2002) 223–246.
[31] M. Lopes, J. Santos-Victor, A developmental roadmap for learning by imitation in robots, IEEE Transactions on Systems, Man, and Cybernetics-Part B: Cybernetics 37 (2) (2007) 159–168.
[32] Webots official website: http://www.cyberbotics.com/.
[33] J. Zagal, J. Ruiz-del-Solar, UCHILSIM: A dynamically and visually realistic simulator for the robocup four legged league, in: RoboCup 2004, in: Lecture Notes in Computer Science, vol. 3276, 2005, pp. 34–45.
[34] Aldebaran robotics official website: http://www.aldebaran-robotics.com/.
[35] URBI official wbesite: http://www.urbiforge.com/.
[36] Fall sequences videos: http://www.robocup.cl/fallingvideos.
[37] Animazoo official website: http://www.animazoo.com/.
[38] J. Ruiz-del-Solar, P. Vallejos, S. Parra- Tsunekawa, J. Testart, R. Asenjo, P. Hevia, C. Vélez, F. Larraín, UChile roadrunners 2008 team description paper, in: RoboCup Symposium 2008, July 15–18, Suzhou, China, 2008 (CD Proceedings).
[39] MOTION PRO X3 Camera: http://www.redlake.com/products/MotionPro/default.aspx.

J. Ruiz-del-Solar received his diploma in Electrical Engineering and the M.S. degree in Electronic Engineering from the Technical University Federico Santa Maria (Chile) in 1991 and 1992, respectively, and the Doctor-Engineer degree from the Technical University of Berlin in 1997. In 1998 he joined the Electrical Engineering Department of the Universidad de Chile of as an Assistant Professor. In 2001 he became Director of the Robotics Laboratory and in 2005 Associate Professor. His research interests include Mobile Robotics, Human-Robot Interaction, and Face Analysis. Dr. Ruiz-del-Solar is recipient of the IEEE RAB Achievement Award 2003, RoboCup Engineering Challenge Award 2004, RoboCup @Home Innovation Award 2007, and RoboCup @Home Innovation Award 2008. Since 2006 he is senior member of the IEEE, and since 2008 Distinguished Lecturer of the IEEE Robotics and Automation Society.

R. Palma-Amestoy received the degree in Electrical Engineer at Universidad de Chile in 2003. He is currently a Ph.D. candidate student for Universidad de Chile, Departamento de Ingeniera Electrica in the field of robotics vision systems.

R. Marchant received the Bachelor degree in Engineering Science at Universidad de Chile in 2008. He is currently an undergraduate Student of Electrical Engineer at Universidad de Chile. He works in the Laboratory of Robotics Systems in the Departamento de Ingeniería Eléctrica at the Universidad de Chile.

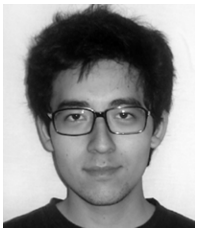

I. Parra Tsunekawa graduated with Highest Honors as Electrical Engineer at the Universidad de Chile, Santiago, Chile, in 2008. He is a member of the Robotics Laboratory at the Department of Electrical Engineering of the Universidad de Chile since 2008. Currently he is a Ph.D. student at the same university. His research interests include robotics, electronic, sensors, autonomous systems, and embedded systems.

P. Zegers received the degree in electrical engineer from the Universidad Catolica and the Ph.D. degree from the University of Arizona. He is currently professor at the Universidad de los Andes, Santiago de Chile.